A Passivity-based Decomposing Method for Operational Space Control of Kinematical Redundant Tele-operation Systems

Kamil Cetin * **Enver Tatlicioglu** **

* *The School of Engineering & Physical Science, Heriot-Watt University, EH14 4AS, Edinburgh, UK (e-mail: k.cetin@hw.ac.uk)*
** *Department of Electrical & Electronics Engineering, Ege University, 35100, Izmir, Turkey (e-mail: enver.tatlicioglu@ege.edu.tr)*

Abstract: In the passivity-based decomposing method, a bilateral tele-operation system is virtually decomposed into 2 sub-systems (shape/locked) to ensure coordination between the master and slave robots and to provide a general referenced motion of the closed-loop bilateral tele-operation along with the passivity of the master and slave robots. So far, the passivity-based decomposing methods in the literature have been studied only for the joint-space control of tele-operation systems with kinematical similar master and slave robots. In this study, a passivity-based decomposing method is proposed for operational space control of bilateral tele-operation systems with kinematic redundancy in the slave robot. The main objectives of the proposed method are to ensure operational space coordination between the robots' end-effector trajectories and to achieve a referenced general movement of the closed-loop tele-operation system. In addition, the kinematic redundancy of the slave robot, which usually complicates the control problem, is turned into an advantage, and secondary tasks are designed for the slave robot. Moreover, experiments are carried out to validate the achievement of the proposed method using a kinematical redundant tele-operation setup.

Keywords: passivity-based decomposing, tele-operation, operational space control, kinematic redundancy, secondary task.

1. INTRODUCTION

In a classical bilateral tele-operation system, which is represented in Fig. 1, the stability of the bilateral tele-operation system should be ensured when the human operator sends control commands to the slave robot via the master robot to perform the tasks given in the remote environment. In addition to the stability, the passivity of the bilateral tele-operation system is an important feature in various bilateral tele-operation applications and ensures that the energy produced by the tele-operation system does not overrun the energy given at the input to the tele-operation system. Besides the stability and passivity, the safety of the remote environment and human operator is also a significant matter in many bilateral tele-operation applications that require precise contact in some areas such as hazardous waste handling and robotic surgery. In short, the passivity and safety ensures safe physical interaction of the slave robot with the remote environment and the human operator with the master robot, and also reduces possible damage to the environment and operator. As (Hokayem and Spong, 2006; Nuno et al., 2011; Chang and Kim, 2012) state in the detailed literature reviews, a large amount of studies has focused on the stability, passivity and safety of bilateral tele-operation systems.

In the literature, there are several passivity-based control methods that help stabilize the bilateral tele-operation systems where the passive operator and the passive environment are interconnected. The passivity-based decomposing approach, which aims to provide both stability and passivity of a comprehensive closed-loop tele-operation system, was first proposed by (Li, 1998), and then they extended this method in their later studies (Li and Lee, 2003; Lee and Li, 2005, 2007; Lee et al., 2013; Durbha and Li, 2019; Lee et al., 2020). Basically, the passivity-based decomposing method provides an energetic passivity by virtually separating the bilateral tele-operation system into 2 sub-systems (shape and locked). Since the passivity-based decomposing approach ensures perfect separation of shape/locked sub-systems, internal tele-operation formation and overall maneuver management can be achieved without any dynamic intervention between them. Perfectly decoupled shape/locked sub-systems can be independently controlled to realize the central maneuver and referenced configuration of the bilateral tele-operation systems. Fundamentally, the shape sub-system measures coordination between the master and slave robots and the locked sub-system states the general movement of the closed-loop tele-operation system. (Li and Lee, 2003) presented a passivity-based bilateral feed-forward control method for dynamically similar tele-operated robot arms. Then, (Lee and Li, 2005) expanded the passivity-based decomposing approach by integrating power scaling and inertial scaling methods for dynamically dissimilar tele-operated robot arms. In (Lee and Li, 2007), this method was applied to the bilateral tele-operation systems having multiple rigid-

bodies. In fact, these authors considered the dissimilarity between the master and slave robots only on the size or strengths of the mechanisms. Considering the extension of the passivity-based decomposing method to the kinematical difference tele-operation systems, (Lee et al., 2013) presented a passive set-position modulation method for the tele-operation control of a master haptic device and slave unmanned aerial vehicles. (Durbha and Li, 2019) applied the passivity-based decomposing method to a bilateral tele-operation between an electric motor actuated haptic device and a pneumatic actuated crawling robot. (Lee et al., 2020) developed the passivity-based decomposing based passive velocity control method for a multi degree-of-freedom (dof) hydraulically actuated device. However, all these passivity-based decomposing methods have been developed based on joint-space control and therefore can only be applied to the kinematical similar tele-operated robot arms in terms of dof or to the kinematical dissimilar tele-operation systems with different actuated mechanisms. One of the motivations of this study stems from the idea that the passivity-based decomposing method can be developed and applied for a bilateral tele-operation system having kinematical dissimilar master and slave robot arms with revolute joints.

In most tele-operation applications, human operators generally use a joystick or non-redundant device as the master robot, and a kinematical redundant robot with more dof than the Cartesian space dimension is often used as the slave robot in the remote environment. To deal with the kinematic dissimilarity between master and slave robots, in the studies of (Courreges et al., 2005; G. Frazelle et al., 2018; Houssem et al., 2018), the authors developed new master robots according to the kinematics of the slave robots. From a control perspective, robots should be controlled in the operational space instead of the joint-space so that the slave robot's end-effector can track the master robot's end-effector position if they have the same Cartesian space dimensions. However, due to an infinite number of solutions for joint formations for any referenced end-effector position, an inverse kinematic problem occurs for the kinematical redundant robot arm. On the other hand, joint motion in the null-space of the Jacobian matrix of the slave robot can be utilized to realize secondary tasks such as referenced joint configurations, maximum dexterity, obstacle avoidance, etc. In the literature Hwang and Hannaford (1998); Nath et al. (2009); Liu and Chopra (2011); Kapadia et al. (2012); Aldana et al. (2018), there are some past works that focused on operational space control of tele-operation systems that have kinematical redundant slave robots. However, all these works targeted the problem of the operational space control and redundancy resolution of the kinematical redundant tele-operation systems, but did not consider the passivity and safety issues in the human robot interaction. This literature review shows that the passivity issue has not been studied sufficiently in detail for the kinematical redundant tele-operation systems.

According to the motivations revealed above, in this study, a passivity-based decomposing method for operational space controller is proposed for the bilateral tele-operation systems having kinematical dissimilar master and slave robot arms. In particular, by using a non-square decom-

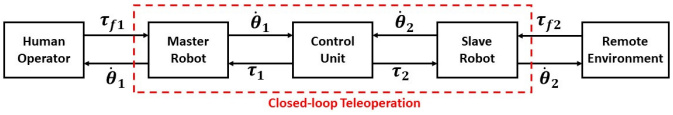

Fig. 1. Representation of closed-loop tele-operation system.

position matrix designed in the operational space, an $(n_1 + n_2)$ dof redundant closed-loop tele-operation system having an n_1 dof non-redundant master robot and an n_2 dof kinematical redundant slave robot where $n_2 > n_1$ is virtually decomposed into 2 n_1 dof sub-systems (shape and locked). The combined operational space controllers for these sub-systems are then designed to allow the end-effector position of the slave robot to track the end-effector position of the master robot in the operational space and achieve the referenced general movement for the closed-loop tele-operation system. The $(n_2 - n_1)$ redundant dof of the slave robot are used by designing a null-space controller to achieve some secondary objectives in the slave robot. Specifically, the so-called pseudo-inverse Jacobian-based technique in (Siciliano, 1990) is used to solve the redundancy resolution. In addition to the operational space control and redundancy solution in the bilateral tele-operation system, the other motivation behind this approach is that the total energy of the bilateral tele-operation system is always equal to or less than the initial stored energy plus the added amount. Since the passive sub-systems of the bilateral tele-operation system cannot produce energy themselves, a robot cannot introduce more energy into a human operator than the controller input during physical human robot interactions. As a result, passivity prevents unlimited growth of the dynamic outputs of the tele-operation system, thereby increasing safety.

The proposed method is based on the dynamic and kinematic models and full-state feed-back along with force measurements of the master and slave robots' end-effectors. It should be noted that the bilateral tele-operation network configuration in this study is based on four channel architecture proposed by (Lawrence, 1993) and used a dedicated communication channel between a computer of master robot and a computer of slave system (e.g. da Vinci's surgical robotic system and ESA telerobotic system (Muradore and Fiorini, 2016)) without any time delay perceptible by a human operator. Experiments are demonstrated to validate the achievement of the proposed method.

2. DYNAMIC AND KINEMATIC MODELS OF MASTER AND SLAVE ROBOTS

From the standard Euler-Lagrange equations in (Lewis et al., 2003), the motion equations in the joint space that describe an n_1 dof master and an n_2 dof slave robots with revolute joints can be given as follows

$$\boldsymbol{M_i}(\boldsymbol{\theta_i})\ddot{\boldsymbol{\theta}}_{\boldsymbol{i}} + \boldsymbol{C_i}(\boldsymbol{\theta_i}, \dot{\boldsymbol{\theta}}_{\boldsymbol{i}})\dot{\boldsymbol{\theta}}_{\boldsymbol{i}} = \boldsymbol{\tau_i} + \boldsymbol{\tau_{f_i}} \tag{1}$$

where the sub-script $i = 1$ represents n_1 dof master robot and the sub-script $i = 2$ represents n_2 dof slave robot. In (1), $\boldsymbol{\theta_i}(t), \dot{\boldsymbol{\theta}}_{\boldsymbol{i}}(t), \ddot{\boldsymbol{\theta}}_{\boldsymbol{i}}(t) \in \mathbb{R}^{n_i}$ denote joint positions, velocities, and accelerations, respectively, $\boldsymbol{M_i}(\boldsymbol{\theta_i}) \in \mathbb{R}^{n_i \times n_i}$ denotes inertia matrices, $\boldsymbol{C_i}(\boldsymbol{\theta_i}, \dot{\boldsymbol{\theta}}_{\boldsymbol{i}}) \in \mathbb{R}^{n_i \times n_i}$ denotes

Coriolis matrices, $\boldsymbol{\tau_i}(t) \in \mathbb{R}^{n_i}$ denotes control input torque vectors, and $\boldsymbol{\tau_{f_1}}(t) \in \mathbb{R}^{n_1}$ is human forces effecting to the master robot's joints and $\boldsymbol{\tau_{f_2}}(t) \in \mathbb{R}^{n_2}$ denotes the forces originating from the remote environment effecting the slave robot's joints. $\boldsymbol{\tau_{f_i}}(t)$ arising from the human and remote environment can be represented in the joint-space as $\boldsymbol{J_i^T \bar{\tau}_{f_i}}$ with $\boldsymbol{J_i}(\boldsymbol{\theta_i}) \in \mathbb{R}^{n_1 \times n_i}$ being yet to be defined as the master/slave robots' Jacobian matrices. $\boldsymbol{\bar{\tau}_{f_i}}(t) \in \mathbb{R}^{n_1}$ refers the forces applied to the robots' end-effectors by the human and environment.

The inertia matrices are symmetric, positive definite and can be limited by the following inequalities

$$m_{1_i} \boldsymbol{I_{n_i}} \leq \boldsymbol{M_i}(\boldsymbol{\theta_i}) \leq m_{2_i} \boldsymbol{I_{n_i}} \tag{2}$$

where m_{1_i}, m_{2_i} are positive constants, and $\boldsymbol{I_{n_i}}$ is the standard $n_i \times n_i$ identity matrix. The symmetric inertia matrix is bounded to minimum constant m_{1_i} and maximum constant m_{2_i} (Lewis et al., 2003). The inertia and Coriolis matrices ensure the skew-symmetric relations

$$\zeta^T [\dot{\boldsymbol{M}}_{\boldsymbol{i}}(\boldsymbol{\theta_i}) - 2\boldsymbol{C_i}(\boldsymbol{\theta_i}, \dot{\boldsymbol{\theta}}_{\boldsymbol{i}})]\zeta = 0 \quad \forall \zeta \in \mathbb{R}^{n_i} \tag{3}$$

where $\dot{\boldsymbol{M}}_{\boldsymbol{i}}(\boldsymbol{\theta_i})$ refers the time derivative of the inertia matrix (Lewis et al., 2003).

For the joint-space representation of $n_1 + n_2$ dof nonlinear tele-operation system, from (1), the coupled dynamic model of master and slave robots can be expressed in an augmented matrix form as in (McIntyre et al., 2006)

$$\begin{bmatrix} \boldsymbol{M_1} & \boldsymbol{0_{n_1 \times n_2}} \\ \boldsymbol{0_{n_2 \times n_1}} & \boldsymbol{M_2} \end{bmatrix} \begin{bmatrix} \ddot{\boldsymbol{\theta}}_{\boldsymbol{1}} \\ \ddot{\boldsymbol{\theta}}_{\boldsymbol{2}} \end{bmatrix} + \begin{bmatrix} \boldsymbol{C_1} & \boldsymbol{0_{n_1 \times n_2}} \\ \boldsymbol{0_{n_2 \times n_1}} & \boldsymbol{C_2} \end{bmatrix} \begin{bmatrix} \dot{\boldsymbol{\theta}}_{\boldsymbol{1}} \\ \dot{\boldsymbol{\theta}}_{\boldsymbol{2}} \end{bmatrix} = \begin{bmatrix} \boldsymbol{\tau_1} \\ \boldsymbol{\tau_2} \end{bmatrix} + \begin{bmatrix} \boldsymbol{\tau_{f_1}} \\ \boldsymbol{\tau_{f_2}} \end{bmatrix} \tag{4}$$

where $\boldsymbol{0_{n_1 \times n_2}} \in \mathbb{R}^{n_1 \times n_2}$, $\boldsymbol{0_{n_2 \times n_1}} \in \mathbb{R}^{n_2 \times n_1}$ are zero matrices.

The kinematical models of the non-redundant master and redundant slave robots are given as

$$\boldsymbol{x_i} = \boldsymbol{f_i}(\boldsymbol{\theta_i}) \tag{5}$$

where $\boldsymbol{x_i}(t) \in \mathbb{R}^{n_1}$ are the end-effector positions in the operational space, $\boldsymbol{f_1} : \mathbb{R}^{n_1} \to \mathbb{R}^{n_1}$ and $\boldsymbol{f_2} : \mathbb{R}^{n_2} \to \mathbb{R}^{n_1}$ denote the forward kinematics of master and slave robots, respectively. Differentiating the forward kinematics in (5) yields

$$\dot{\boldsymbol{x}}_{\boldsymbol{i}} = \boldsymbol{J_i} \dot{\boldsymbol{\theta}}_{\boldsymbol{i}} \tag{6}$$

where $\boldsymbol{J_1}(\boldsymbol{\theta_1}) \triangleq \frac{\partial \boldsymbol{f_1}}{\partial \boldsymbol{\theta_1}} \in \mathbb{R}^{n_1 \times n_1}$ is the Jacobian matrix of the master robot and $\boldsymbol{J_2}(\boldsymbol{\theta_2}) \triangleq \frac{\partial \boldsymbol{f_2}}{\partial \boldsymbol{\theta_2}} \in \mathbb{R}^{n_1 \times n_2}$ is the Jacobian matrix of the slave robot.

After setting the slave robot's null-space velocity to zero in (6), the general solutions for the velocity kinematics can be obtained as

$$\dot{\boldsymbol{\theta}}_{\boldsymbol{1}} = \boldsymbol{J_1}^{-1} \dot{\boldsymbol{x}}_{\boldsymbol{1}} \tag{7}$$

$$\dot{\boldsymbol{\theta}}_{\boldsymbol{2}} = \boldsymbol{J_2}^{+} \dot{\boldsymbol{x}}_{\boldsymbol{2}} \tag{8}$$

where $\boldsymbol{J_2}^{+}(\boldsymbol{\theta_2}) \in \mathbb{R}^{n_2 \times n_1}$ is the slave robot's pseudo-inversed Jacobian matrix as

$$\boldsymbol{J_2}^{+} \triangleq \boldsymbol{J_2}^T (\boldsymbol{J_2 J_2}^T)^{-1} \tag{9}$$

which satisfies

$$\boldsymbol{J_2 J_2}^{+} = \boldsymbol{I_{n_1}}. \tag{10}$$

The pseudo-inversed Jacobian matrix $\boldsymbol{J_2}^{+}$ satisfies the Moore-Penrose conditions in (Rao and Mitra, 1971). Differentiating the velocity kinematics one more time yields

$$\ddot{\boldsymbol{x}}_{\boldsymbol{i}} = \dot{\boldsymbol{J}}_{\boldsymbol{i}} \dot{\boldsymbol{\theta}}_{\boldsymbol{i}} + \boldsymbol{J_i} \ddot{\boldsymbol{\theta}}_{\boldsymbol{i}}. \tag{11}$$

From the acceleration kinematics in (11), via utilizing the velocity kinematics in (6) with the general solutions in (7) and (8), the joint accelerations of the master and slave robots are obtained as follows

$$\ddot{\boldsymbol{\theta}}_{\boldsymbol{1}} = \boldsymbol{J_1}^{-1} \ddot{\boldsymbol{x}}_{\boldsymbol{1}} - \boldsymbol{J_1}^{-1} \dot{\boldsymbol{J}}_{\boldsymbol{1}} \boldsymbol{J_1}^{-1} \dot{\boldsymbol{x}}_{\boldsymbol{1}} \tag{12}$$

$$\ddot{\boldsymbol{\theta}}_{\boldsymbol{2}} = \boldsymbol{J_2}^{+} \ddot{\boldsymbol{x}}_{\boldsymbol{2}} - \boldsymbol{J_2}^{+} \dot{\boldsymbol{J}}_{\boldsymbol{2}} \boldsymbol{J_2}^{+} \dot{\boldsymbol{x}}_{\boldsymbol{2}} \tag{13}$$

where minimum norm acceleration solution for the slave robot is obtained by setting the null-space acceleration to zero.

Following assumptions 1 and 2 are standard in robot control literature (Spong and Vidyasagar, 1989; Lewis et al., 2003).

Assumption 1. In the control development, it is assumed that the $\boldsymbol{J_1}(\boldsymbol{\theta_1})$, $\boldsymbol{J_2}(\boldsymbol{\theta_2})$, $\boldsymbol{J_1}^{-1}(\boldsymbol{\theta_1})$ and $\boldsymbol{J_2}^{+}(\boldsymbol{\theta_2})$ depend on all possible joint positions $\boldsymbol{\theta_i}(t)$ only as arguments of sinusoidal functions and all kinematic singularities on both master and slave robots are always avoided.

Assumption 2. The kinematic and dynamic equations depend on $\boldsymbol{\theta_i}(t)$ only through trigonometrical functions and hereby they remain within the limits for all possible $\boldsymbol{\theta_i}(t)$.

Assumption 3. The closed-loop tele-operation in Fig. 1 ensures the energetic passivity state with a constant $b \in \mathbb{R}$ and the sum of human power and environment power $\forall t \geq 0$ (Lee, 2004)

$$\int_0^t \left(\boldsymbol{\tau_{f_1}}^T(\sigma) \dot{\boldsymbol{\theta}}_{\boldsymbol{1}}(\sigma) + \boldsymbol{\tau_{f_2}}^T(\sigma) \dot{\boldsymbol{\theta}}_{\boldsymbol{2}}(\sigma) \right) d\sigma \geq -b^2. \tag{14}$$

Assuming admittance causality for the closed-loop tele-operation system shown in Fig. 1, the energetic passivity state (14) indicates that the closed-loop tele-operation is passive with the inputs $(\boldsymbol{\tau_{f_1}}, \boldsymbol{\tau_{f_2}})$ and the outputs $(\dot{\boldsymbol{\theta}}_{\boldsymbol{1}}, \dot{\boldsymbol{\theta}}_{\boldsymbol{2}})$ and that the maximum energy extracted from the closed-loop tele-operation is limited at all times (Lozano et al., 2000).

Assumption 4. The controller in Fig. 1 satisfies the controller's passivity state with a constant $c \in \mathbb{R}$ and the sum of master control power and slave control power $\forall t \geq 0$ (Lee, 2004)

$$\int_0^t \left(\boldsymbol{\tau_1}^T(\sigma) \dot{\boldsymbol{\theta}}_{\boldsymbol{1}}(\sigma) + \boldsymbol{\tau_2}^T(\sigma) \dot{\boldsymbol{\theta}}_{\boldsymbol{2}}(\sigma) \right) d\sigma \leq c^2. \tag{15}$$

Assuming impedance causality for the master and slave robots shown in Fig. 1, the controller's passivity state (15) indicates that the controller is passive with the inputs $(\dot{\boldsymbol{\theta}}_{\boldsymbol{1}}, \dot{\boldsymbol{\theta}}_{\boldsymbol{2}})$ and the outputs $(\boldsymbol{\tau_1}, \boldsymbol{\tau_2})$ and that the maximum energy generated from the controller is always bounded (Lozano et al., 2000).

Proposition 5. For the dynamic model of the closed-loop tele-operation system (1), the controller's passivity state (15) refers to the energetic passivity (14) (Lee, 2004).

Proof. The total kinetic energy of the closed-loop tele-operation system is defined as

$$E_k(t) \triangleq \frac{1}{2} \dot{\boldsymbol{\theta}}_{\boldsymbol{1}}^T(t) \boldsymbol{M_1}(\boldsymbol{\theta_1}) \dot{\boldsymbol{\theta}}_{\boldsymbol{1}}(t) + \frac{1}{2} \dot{\boldsymbol{\theta}}_{\boldsymbol{2}}^T(t) \boldsymbol{M_2}(\boldsymbol{\theta_2}) \dot{\boldsymbol{\theta}}_{\boldsymbol{2}}(t) \tag{16}$$

utilizing the dynamic models of the master and slave in (1) with the property in (3). Taking the time derivative of (16), it is obtained

$$\dot{E}_k(t) = (\boldsymbol{\tau_1}(t) + \boldsymbol{\tau_{f_1}}(t))^T \dot{\boldsymbol{\theta}}_{\mathbf{1}}(t) + (\boldsymbol{\tau_2}(t) + \boldsymbol{\tau_{f_2}}(t))^T \dot{\boldsymbol{\theta}}_{\mathbf{2}}(t). \tag{17}$$

Integrating the equation (17) and substituting the controller's passivity state (15) into that, it is obtained

$$\int_0^t \left(\boldsymbol{\tau_{f_1}}^T(\sigma) \dot{\boldsymbol{\theta}}_{\mathbf{1}}(\sigma) + \boldsymbol{\tau_{f_2}}^T(\sigma) \dot{\boldsymbol{\theta}}_{\mathbf{2}}(\sigma) \right) d\sigma \geq -E_k(0) - c^2 := -b^2. \tag{18}$$

This result shows that the closed-loop tele-operation system is energetically passive after carefully analyzing the controller's passivity state (15) (Lee, 2004).

3. DECOMPOSITION IN OPERATIONAL SPACE

There are two design objectives for the decomposition of the redundant tele-operation system model into 2 n_1 dof sub-systems: 1) shape sub-system provides coordination between the master and slave robots' end-effector positions, 2) locked sub-system ensures a referenced general movement for the closed-loop tele-operation system. According to these design objectives, a non-square decomposition matrix $\boldsymbol{S}(\boldsymbol{\theta_1}, \boldsymbol{\theta_2}) \in \mathbb{R}^{2n_1 \times (n_1+n_2)}$ is defined as follows

$$\boldsymbol{S} \triangleq \begin{bmatrix} (\boldsymbol{I}_{n_1} - \bar{\boldsymbol{\Phi}})\, \boldsymbol{J_1} & \bar{\boldsymbol{\Phi}} \boldsymbol{J_2} \\ \boldsymbol{J_1} & -\boldsymbol{J_2} \end{bmatrix} \tag{19}$$

where $\bar{\boldsymbol{\Phi}}\,(\boldsymbol{x_1}, \boldsymbol{x_2}) \in \mathbb{R}^{n_1 \times n_1}$ is defined as

$$\bar{\boldsymbol{\Phi}} \triangleq \left(\bar{\boldsymbol{M}}_{\mathbf{2}}{}^{-1} \bar{\boldsymbol{M}}_{\mathbf{1}} + \boldsymbol{I}_{n_1} \right)^{-1} \tag{20}$$

where $\bar{\boldsymbol{M}}_{\mathbf{1}}(\boldsymbol{\theta_1}), \bar{\boldsymbol{M}}_{\mathbf{2}}(\boldsymbol{\theta_2}) \in \mathbb{R}^{n_1 \times n_1}$ denote the master and slave robots' inertia matrices in the operational space defined as

$$\bar{\boldsymbol{M}}_{\mathbf{1}} \triangleq \boldsymbol{J_1}^{-T} \boldsymbol{M_1} \boldsymbol{J_1}^{-1} \tag{21}$$

$$\bar{\boldsymbol{M}}_{\mathbf{2}} \triangleq \boldsymbol{J_2}^{+T} \boldsymbol{M_2} \boldsymbol{J_2}^{+}. \tag{22}$$

The decomposition matrix transforms the closed-loop tele-operation system equations from joint-space to operational space as

$$\begin{bmatrix} \dot{\boldsymbol{x}}_{\boldsymbol{L}} \\ \dot{\boldsymbol{x}}_{\boldsymbol{E}} \end{bmatrix} = \boldsymbol{S} \begin{bmatrix} \dot{\boldsymbol{\theta}}_{\mathbf{1}} \\ \dot{\boldsymbol{\theta}}_{\mathbf{2}} \end{bmatrix} \tag{23}$$

where $\dot{\boldsymbol{x}}_{\boldsymbol{L}}(t) \in \mathbb{R}^{n_1}$ represents the weighted mean velocity of the master and slave robots in the operational space and $\dot{\boldsymbol{x}}_{\boldsymbol{E}}(t) \in \mathbb{R}^{n_1}$ is the coordination error velocity in the operational space. Since the $(n_1 + n_2)$ dof closed-loop tele-operation system is redundant, the pseudo-inversed decomposition matrix $\boldsymbol{S}^{+}(\boldsymbol{\theta_1}, \boldsymbol{\theta_2}) \in \mathbb{R}^{(n_1+n_2) \times 2n_1}$ is defined as

$$\boldsymbol{S}^{+} \triangleq \boldsymbol{S}^T (\boldsymbol{S}\boldsymbol{S}^T)^{-1} \tag{24}$$

is used to convert the coupled dynamic equations from the joint-space to the operational space. The coupled dynamics in (4) are then transformed into the operational space by using the transformation matrices in (23) and (24)as

$$\begin{bmatrix} \bar{\boldsymbol{M}}_{\boldsymbol{L}} & \boldsymbol{0}_{n_1 \times n_1} \\ \boldsymbol{0}_{n_1 \times n_1} & \bar{\boldsymbol{M}}_{\boldsymbol{E}} \end{bmatrix} \begin{bmatrix} \ddot{\boldsymbol{x}}_{\boldsymbol{L}} \\ \ddot{\boldsymbol{x}}_{\boldsymbol{E}} \end{bmatrix} + \begin{bmatrix} \bar{\boldsymbol{C}}_{\boldsymbol{L}} & \bar{\boldsymbol{C}}_{\boldsymbol{LE}} \\ \bar{\boldsymbol{C}}_{\boldsymbol{EL}} & \bar{\boldsymbol{C}}_{\boldsymbol{E}} \end{bmatrix} \begin{bmatrix} \dot{\boldsymbol{x}}_{\boldsymbol{L}} \\ \dot{\boldsymbol{x}}_{\boldsymbol{E}} \end{bmatrix} = \begin{bmatrix} \boldsymbol{\tau_L} \\ \boldsymbol{\tau_E} \end{bmatrix} + \begin{bmatrix} \boldsymbol{\tau_{f_L}} \\ \boldsymbol{\tau_{f_E}} \end{bmatrix} \tag{25}$$

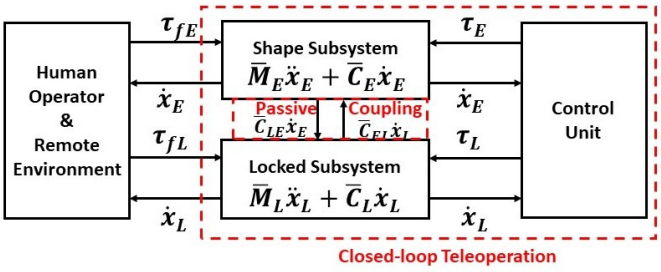

Fig. 2. The decomposed closed-loop tele-operation system.

where $\bar{\boldsymbol{M}}_{\boldsymbol{E}}(t)$, $\bar{\boldsymbol{M}}_{\boldsymbol{L}}(t)$, $\bar{\boldsymbol{C}}_{\boldsymbol{LE}}(t)$, $\bar{\boldsymbol{C}}_{\boldsymbol{L}}(t)$, $\bar{\boldsymbol{C}}_{\boldsymbol{E}}(t)$, $\bar{\boldsymbol{C}}_{\boldsymbol{EL}}(t) \in \mathbb{R}^{n_1 \times n_1}$ and $\boldsymbol{\tau_{f_L}}(t)$, $\boldsymbol{\tau_{f_E}}(t)$, $\boldsymbol{\tau_L}(t)$, $\boldsymbol{\tau_E}(t) \in \mathbb{R}^{n_1}$ are obtained from

$$\begin{bmatrix} \bar{\boldsymbol{M}}_{\boldsymbol{L}} & \boldsymbol{0}_{n_1 \times n_1} \\ \boldsymbol{0}_{n_1 \times n_1} & \bar{\boldsymbol{M}}_{\boldsymbol{E}} \end{bmatrix} \triangleq \boldsymbol{S}^{+T} \begin{bmatrix} \boldsymbol{M_1} & \boldsymbol{0}_{n_1 \times n_2} \\ \boldsymbol{0}_{n_2 \times n_1} & \boldsymbol{M_2} \end{bmatrix} \boldsymbol{S}^{+} \tag{26}$$

$$\begin{bmatrix} \bar{\boldsymbol{C}}_{\boldsymbol{L}} & \bar{\boldsymbol{C}}_{\boldsymbol{LE}} \\ \bar{\boldsymbol{C}}_{\boldsymbol{EL}} & \bar{\boldsymbol{C}}_{\boldsymbol{E}} \end{bmatrix} \triangleq \boldsymbol{S}^{+T} \begin{bmatrix} \boldsymbol{C_1} & \boldsymbol{0}_{n_1 \times n_2} \\ \boldsymbol{0}_{n_2 \times n_1} & \boldsymbol{C_2} \end{bmatrix} \boldsymbol{S}^{+} - \boldsymbol{S}^{+T} \begin{bmatrix} \boldsymbol{M_1} & \boldsymbol{0}_{n_1 \times n_2} \\ \boldsymbol{0}_{n_2 \times n_1} & \boldsymbol{M_2} \end{bmatrix} \boldsymbol{S}^{+} \dot{\boldsymbol{S}} \boldsymbol{S}^{+} \tag{27}$$

$$\begin{bmatrix} \boldsymbol{\tau_{f_L}} \\ \boldsymbol{\tau_{f_E}} \end{bmatrix} \triangleq \boldsymbol{S}^{+T} \begin{bmatrix} \boldsymbol{\tau_{f_1}} \\ \boldsymbol{\tau_{f_2}} \end{bmatrix} \tag{28}$$

$$\begin{bmatrix} \boldsymbol{\tau_L} \\ \boldsymbol{\tau_E} \end{bmatrix} \triangleq \boldsymbol{S}^{+T} \begin{bmatrix} \boldsymbol{\tau_1} \\ \boldsymbol{\tau_2} \end{bmatrix}. \tag{29}$$

The decomposed closed-loop tele-operation system is represented in Fig. 2. From (25), the dynamic models of the shape/locked sub-systems can be separately written as

$$\bar{\boldsymbol{M}}_{\boldsymbol{L}} \ddot{\boldsymbol{x}}_{\boldsymbol{L}} + \bar{\boldsymbol{C}}_{\boldsymbol{L}} \dot{\boldsymbol{x}}_{\boldsymbol{L}} + \bar{\boldsymbol{C}}_{\boldsymbol{LE}} \dot{\boldsymbol{x}}_{\boldsymbol{E}} = \boldsymbol{\tau_L} + \boldsymbol{\tau_{f_L}} \tag{30}$$

$$\bar{\boldsymbol{M}}_{\boldsymbol{E}} \ddot{\boldsymbol{x}}_{\boldsymbol{E}} + \bar{\boldsymbol{C}}_{\boldsymbol{E}} \dot{\boldsymbol{x}}_{\boldsymbol{E}} + \bar{\boldsymbol{C}}_{\boldsymbol{EL}} \dot{\boldsymbol{x}}_{\boldsymbol{L}} = \boldsymbol{\tau_E} + \boldsymbol{\tau_{f_E}}. \tag{31}$$

4. DESIGN OF CONTROLLERS

Depending on the dynamic model of the shape sub-system in (31), the controller of the shape sub-system $\boldsymbol{\tau_E}(t)$ is designed as

$$\boldsymbol{\tau_E} = \bar{\boldsymbol{C}}_{\boldsymbol{EL}} \dot{\boldsymbol{x}}_{\boldsymbol{L}} - \boldsymbol{K_v} \dot{\boldsymbol{x}}_{\boldsymbol{E}} - \boldsymbol{K_p} \boldsymbol{x_E} - \boldsymbol{\tau_{f_E}} \tag{32}$$

where $\boldsymbol{K_v}$, $\boldsymbol{K_p} \in \mathbb{R}^{n_1 \times n_1}$ are positive definite, diagonal, constant control gain matrices. When (32) is substituted into (31), the closed-loop dynamics of the shape sub-system is obtained as

$$\bar{\boldsymbol{M}}_{\boldsymbol{E}} \ddot{\boldsymbol{x}}_{\boldsymbol{E}} + \bar{\boldsymbol{C}}_{\boldsymbol{E}} \dot{\boldsymbol{x}}_{\boldsymbol{E}} + \boldsymbol{K_v} \dot{\boldsymbol{x}}_{\boldsymbol{E}} + \boldsymbol{K_p} \boldsymbol{x_E} = \boldsymbol{0}_{n_1 \times 1} \tag{33}$$

where it can be clearly seen that the controller aim for the shape sub-system is ensured in the following state

$$\boldsymbol{x_E} = \boldsymbol{x_1} - \boldsymbol{x_2} \to 0 \Leftrightarrow \boldsymbol{x_2} \to \boldsymbol{x_1} \tag{34}$$

where perfect coordination between the master and slave robots' end-effector positions is achieved.

Considering the general referenced movement of the closed-loop tele-operation system, for the aim of that the locked sub-system dynamics tracks an operational space trajectory produced from human/environment combined forces, the controller of the locked sub-system is designed as

$$\boldsymbol{\tau_L} = \bar{\boldsymbol{C}}_{\boldsymbol{LE}} \dot{\boldsymbol{x}}_{\boldsymbol{E}}. \tag{35}$$

Substituting (35) into (30) results in

$$\bar{\boldsymbol{M}}_{\boldsymbol{L}} \ddot{\boldsymbol{x}}_{\boldsymbol{L}} + \bar{\boldsymbol{C}}_{\boldsymbol{L}} \dot{\boldsymbol{x}}_{\boldsymbol{L}} = \boldsymbol{\tau_{f_L}} \tag{36}$$

thus the second control objective is achieved.

It should be especially noticed that the n_1+n_2 dof closed-loop tele-operation system having n_1 dof master and n_2 dof slave systems are the physical systems, but n_1 dof shape and n_1 dof locked decomposed sub-systems are not physical systems. Therefore, the designed controllers in (32) and (35) for the shape/locked sub-systems, respectively, are not directly applied to the physical sub-systems of the closed-loop tele-operation. By using the decomposition matrix as shown in the equation of (29), the designed controllers (32) and (35) are converted to the control input torques $\boldsymbol{\tau_1}$ and $\boldsymbol{\tau_2}$ and applied to the master and slave systems, respectively, under the Assumptions 1 and 2.

Taking the advantage of kinematically redundancy of the slave robot, a secondary task can be achieved. For the secondary task, a modified control input torque, denoted by $\underline{\boldsymbol{\tau_2}}(t) \in \mathbb{R}^{n_2}$, is developed by integrating $\boldsymbol{\tau_2}(t)$ with a null-space control input $\boldsymbol{\tau_{null}}(\boldsymbol{\theta_2}) \in \mathbb{R}^{n_2}$ as

$$\underline{\boldsymbol{\tau_2}} = \boldsymbol{\tau_2} + (\boldsymbol{I_{n_2}} - \boldsymbol{J_2}^{+}\boldsymbol{J_2})\boldsymbol{\tau_{null}}. \tag{37}$$

Here, $(\boldsymbol{I_{n_2}} - \boldsymbol{J_2}^{+}\boldsymbol{J_2})$ refers a null-space orthogonal projection matrix of $\boldsymbol{J_2}$. In (Nakanishi et al., 2008), most of the redundant solution methods use the null-space projecting approach. The null-space control input can be developed as

$$\boldsymbol{\tau_{null}} = -\boldsymbol{K_{null}}\nabla \boldsymbol{g} \tag{38}$$

where $\boldsymbol{K_{null}} \in \mathbb{R}^{n_2 \times n_2}$ is a positive definite, diagonal, constant control gain matrix, and $\nabla \boldsymbol{g} \in \mathbb{R}^{n_2}$ represents the gradient of a scalar differentiable secondary task function $g(\boldsymbol{\theta_2}) \in \mathbb{R}$ of the kinematically redundant slave robot. The secondary task function is written in terms of a cost function of the joint positions to optimize the secondary objective of the slave robot such as a tracking of the referenced joint configuration.

5. EXPERIMENT

To demonstrate the validity of the proposed approach, an experiment study is performed by using a 2-dof revolute joint arm for the non-redundant master robot and the dynamic and kinematic models of a 3-dof revolute joint arm for the redundant virtual slave. Both robot arms are considered to move in the 2D plane. The computer of the master robot is directly connected to the computer of the virtual slave system via a dedicated communication network port. As indicated in Fig. 1, the control unit sends the designed controllers to the master robot and virtual system and receives the joint measurements and force feed-backs from the master robot and slave system. The force feed-backs are received from the interactions of the human operator with the master robot and the virtual plane with the virtual slave system. PHANToM Omni haptic arm shown in Fig. 3 is used as the master robot, with the highlighted technical specifications of a nominal position resolution of 0.055 mm, a weight of 3 lbs 15 oz, maximum pull/push force nominal of 3.3 N, backdrive friction of 0.26 N, constant pull/push force of 0.88 N. The device has 2 links, 3 active joints. The arm produces haptic force feed-back on X, Y, and Z in the translational directions. PHANToM Omni haptic arm has 3-dof translational positions in the operational space. As the experimental study requires a non-redundant robot arm for the master robot, the first joint of PHANToM arm was mechanically fixed and the last 2 joints with 2 links $l_{1.1}$ and $l_{1.2}$ were used to make a 2-dof robot arm. Therefore, only the joint angles of $\boldsymbol{\theta_1}$ and $\boldsymbol{\theta_2}$ and motions in the X and Y operational space directions were used in the kinematic and dynamic models as can be seen from Fig. 3. For the communication network between the arm and a computer, a local area network was established. Experimental studies were carried out in MATLAB Simulink at 100 Hz data rate. In the master robot's computer, Quarc Library's PHANToM Toolbox in MATLAB/Simulink is used to command the torque control inputs to the PHANToM arm and to measure the joint positions from the arm's digital encoders.

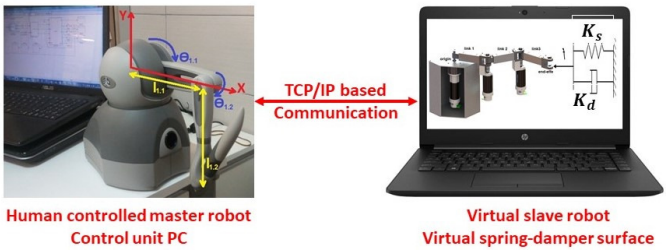

Fig. 3. Representation of the experimental study.

From PHANToM arm's dynamic model, the inertia matrix $\boldsymbol{M_1}(\boldsymbol{\theta_1}) \in \mathbb{R}^{2\times 2}$ and the Coriolis matrix $\boldsymbol{C_1}(\boldsymbol{\theta_1}, \dot{\boldsymbol{\theta}}_1) \in \mathbb{R}^{2\times 2}$ can be given as (Nygaard, 2008)

$$\boldsymbol{M_1} = \begin{bmatrix} M_{1.11} & M_{1.12} \\ M_{1.12} & M_{1.22} \end{bmatrix} \tag{39}$$

$$\boldsymbol{C_1} = \begin{bmatrix} 0 & C_{1.12} \\ C_{1.12} & 0 \end{bmatrix}. \tag{40}$$

where their entries are given as

$$\begin{aligned} M_{1.11} &= k_3 \\ M_{1.12} &= k_2 - 0.5k_1 \sin(\theta_{1.1} - \theta_{1.2}) \\ M_{1.22} &= k_4 \\ C_{1.12} &= 0.25k_1(\dot{\theta}_{1.1} - \dot{\theta}_{1.2}) \cos(\theta_{1.1} - \theta_{1.2}). \end{aligned}$$

In the above expressions, the constant parameters are given as

$$\begin{aligned} k_1 &= 2.766 \times 10^{-3}\text{Kg.m}^2 \quad k_3 = 2.526 \times 10^{-3}\text{Kg.m}^2 \\ k_2 &= 0.308 \times 10^{-3}\text{Kg.m}^2 \quad k_4 = 1.652 \times 10^{-3}\text{Kg.m}^2. \end{aligned} \tag{41}$$

After applying Denavit-Hartenberg convention (Spong and Vidyasagar, 1989), PHANToM arm's end-effector position can then be given as (Nygaard, 2008)

$$\boldsymbol{x_1}(t) = \begin{bmatrix} X(t) \\ Y(t) \end{bmatrix} = \begin{bmatrix} -l_{1.2}c_{1.2} + l_{1.1}s_{1.1} + l_{1.x} \\ l_{1.1}c_{1.1} + l_{1.2}s_{1.2} - l_{1.y} \end{bmatrix} \text{(m)} \tag{42}$$

where $c_{1.i} = \cos(\theta_{1.i})$, $s_{1.i} = \sin(\theta_{1.i})$ were used for $i \in \{2, 3\}$, $l_{1.1} = 0.133$ m, $l_{1.2} = 0.133$ m, $l_{1.x} = 0.023$ m, $l_{1.y} = 0.168$ m. In (42), $l_{1.1}$ and $l_{1.2}$ refer the first link length and the second link length, respectively, and $l_{1.x}$ and $l_{1.y}$ represent transformation off-sets between the first joint and the origin of the end-effector in the operational space.

For redundant slave system, the virtual model of a 3-dof robot arm was implemented in MATLAB/Simulink in the slave system's computer. The model has the following inertia matrix $\boldsymbol{M_2}(\boldsymbol{\theta_2}) \in \mathbb{R}^{3\times 3}$ and Coriolis matrix $\boldsymbol{C_2}(\boldsymbol{\theta_2}, \dot{\boldsymbol{\theta}}_2) \in \mathbb{R}^{3\times 3}$

$$\boldsymbol{M_2} = \begin{bmatrix} M_{2.11} & M_{2.12} & M_{2.13} \\ M_{2.12} & M_{2.22} & M_{2.23} \\ M_{2.13} & M_{2.23} & M_{2.33} \end{bmatrix} \tag{43}$$

$$\boldsymbol{C_2} = \begin{bmatrix} C_{2.11} & C_{2.12} & C_{2.13} \\ C_{2.21} & C_{2.22} & C_{2.23} \\ C_{2.31} & C_{2.32} & C_{2.33} \end{bmatrix} \tag{44}$$

where their entries are given as

$$\begin{aligned} M_{2.11} &= p_1 c_{2.2} + p_2(c_{2.3} + c_{2.23}) + p_3 \\ M_{2.12} &= p_6 c_{2.2} + p_2 c_{2.3} + p_7 c_{2.23} + p_4 \\ M_{2.13} &= p_7(c_{2.3} + c_{2.23}) \\ M_{2.22} &= p_2 c_{2.3} + p_4 \\ M_{2.23} &= p_7 c_{2.3} + p_5 \\ M_{2.33} &= p_5. \end{aligned}$$

$$\begin{aligned} C_{2.11} &= -(p_1 s_{2.2} + p_2 s_{2.23})\dot{\theta}_{2.2} - p_2(s_{2.3} + s_{2.23})\dot{\theta}_{2.3} \\ C_{2.12} &= -(p_6 s_{2.2} + p_7 s_{2.23})\dot{\theta}_{2.2} - p_2(s_{2.3} + s_{2.23})\dot{\theta}_{2.3} \\ C_{2.13} &= -p_7(s_{2.3} + s_{2.23})\dot{\theta}_{2.3} \\ C_{2.21} &= (p_6 s_{2.2} + p_7 s_{2.23})\dot{\theta}_{2.1} \\ C_{2.22} &= -p_2 s_{2.3}\dot{\theta}_{2.3} \\ C_{2.23} &= -p_2 s_{2.3}\dot{\theta}_{2.1} - p_7 s_{2.3}\dot{\theta}_{2.3} \\ C_{2.31} &= p_7(s_{2.3} + s_{2.23})\dot{\theta}_{2.1} \\ C_{2.32} &= p_2 s_{2.3}\dot{\theta}_{2.1} + p_7 s_{2.3}\dot{\theta}_{2.2} \\ C_{2.33} &= 0 \end{aligned}$$

where $s_{2.i}$, $c_{2.i}$, $s_{2.ij}$, $c_{2.ij}$ denote $\sin(\theta_{2.i})$, $\cos(\theta_{2.i})$, $\sin(\theta_{2.i}+\theta_{2.j})$, $\cos(\theta_{2.i}+\theta_{2.j})$ $(i,j \in \{1,2,3\})$, respectively, and p_i $(i \in \{1,...,7\})$ represent constant parameters (*i.e.*, lengths and masses of the links and center mass of each link) with the following values in the unit of $\mathrm{Kg\,m^2}$

$$\begin{aligned} p_1 &= 0.0213 \quad p_5 = 0.0017 \\ p_2 &= 0.0029 \quad p_6 = 0.0106 \\ p_3 &= 0.0433 \quad p_7 = 0.0015 \\ p_4 &= 0.0177. \end{aligned} \tag{45}$$

The virtual slave's end-effector position can be written as

$$\boldsymbol{x_2}(t) = \begin{bmatrix} X(t) \\ Y(t) \end{bmatrix} = \begin{bmatrix} l_{2.1}c_{2.1} + l_{2.2}c_{2.12} + l_{2.3}c_{2.123} \\ l_{2.1}s_{2.1} + l_{2.2}s_{2.12} + l_{2.3}s_{2.123} \end{bmatrix} (\mathrm{m}) \tag{46}$$

where there link lengths $l_{2.1}$, $l_{2.2}$, $l_{2.3}$ are equal to 0.127 m, and $c_{2.123} \triangleq \cos(\theta_{2.1}+\theta_{2.2}+\theta_{2.3})$, $s_{2.123} \triangleq \sin(\theta_{2.1}+\theta_{2.2}+\theta_{2.3})$.

Since there was no torque sensor to measure of external torques acting on the master robot arm by the human operator, a torque observer was developed to estimate them. In development of the torque observer, from (1), the joint acceleration equation can be obtained as

$$\ddot{\boldsymbol{\theta}}_{\mathbf{1}} = {\boldsymbol{M_1}}^{-1}(\boldsymbol{\tau_1} - \boldsymbol{C_1}\dot{\boldsymbol{\theta}}_{\mathbf{1}}) + {\boldsymbol{M_1}}^{-1}\boldsymbol{\tau_{f_1}}. \tag{47}$$

The estimation term of the joint acceleration $\hat{\ddot{\boldsymbol{\theta}}}_{\mathbf{1}}(t) \in \mathbb{R}^2$ is developed as

$$\hat{\ddot{\boldsymbol{\theta}}}_{\mathbf{1}} = \boldsymbol{M_1^{-1}}(\boldsymbol{\tau_1} - \boldsymbol{C_1}\dot{\boldsymbol{\theta}}_{\mathbf{1}}) + \hat{\boldsymbol{\tau}}_{\boldsymbol{F_1}} \tag{48}$$

where $\hat{\boldsymbol{\tau}}_{\boldsymbol{F_1}}(t) \in \mathbb{R}^2$ represents the observer for the vector ${\boldsymbol{M_1}}^{-1}\boldsymbol{\tau_{f_1}}$. The joint velocity estimation error $\boldsymbol{e_f}(t) \in \mathbb{R}^2$ is developed as

$$\boldsymbol{e_f} \triangleq \dot{\boldsymbol{\theta}}_{\mathbf{1}} - \hat{\dot{\boldsymbol{\theta}}}_{\mathbf{1}}. \tag{49}$$

The torque observer is designed as

$$\begin{aligned} \hat{\boldsymbol{\tau}}_{\boldsymbol{F_1}} &= (\boldsymbol{K_f} + \boldsymbol{I_2})(\boldsymbol{e_f}(t) + \int_0^t \boldsymbol{e_f}(\sigma)d\sigma) \\ &+ \boldsymbol{K_l}\int_0^t \mathrm{Tanh}(\boldsymbol{e_f}(\sigma))d\sigma \end{aligned} \tag{50}$$

where $\boldsymbol{K_f}, \boldsymbol{K_l} \in \mathbb{R}^{2\times 2}$ are constant, diagonal, positive definite gain matrices for the observer and $\mathrm{Tanh}(\cdot) \in \mathbb{R}^2$ denotes the tangent hyperbolic function. If $\boldsymbol{K_f}$ and $\boldsymbol{K_l}$ are selected appropriately $\hat{\boldsymbol{\tau}}_{\boldsymbol{F_1}}$ closes to the neighbourhood of ${\boldsymbol{M_1}}^{-1}\boldsymbol{\tau_{f_1}}$ as in (Dasdemir and Zergeroglu, 2015).

In order to produce an environmental force affecting the virtual slave system, the virtual plane was designed using the spring-damper model $\boldsymbol{f_{sd}} \in \mathbb{R}^2$ below

$$\boldsymbol{f_{sd}} = \boldsymbol{K_s}\boldsymbol{x^*} + \boldsymbol{K_d}\dot{\boldsymbol{x}}^* \tag{51}$$

where $\boldsymbol{K_s} \in \mathbb{R}^{2\times 2}$ and $\boldsymbol{K_d} \in \mathbb{R}^{2\times 2}$ are positive definite, diagonal, constant gain matrices for the spring and damper, respectively, and $\boldsymbol{x^*} \in \mathbb{R}^2$ and $\dot{\boldsymbol{x}}^* \in \mathbb{R}^2$ are the penetration depth and speed of the virtual slave's end-effector inside the virtual plane, respectively. The torque applied on the slave robot's joints can be described as

$$\boldsymbol{\tau_{f_2}} = {\boldsymbol{J_2}}^T\boldsymbol{f_{sd}}. \tag{52}$$

The secondary task function $\boldsymbol{g} = (\theta_{2.2} - \theta_{2.3})^2$ which aims that the second joint $\theta_{2.2}$ and the third joint $\theta_{2.3}$ have always the same positions was selected for the redundant slave robot.

For the controller in (32), gain matrices were selected as $\boldsymbol{K_v} = \mathrm{diag}[15;10]\,\mathrm{N\,s}$ and $\boldsymbol{K_p} = \mathrm{diag}[7.5;5]\,\mathrm{N}$. Initial joint positions of the master and slave robots were configured as $\boldsymbol{\theta_1}(0) = [0.26, -0.37]\,\mathrm{rad}$ and $\boldsymbol{\theta_2}(0) = [1.57; 1.57; 1.57]\,\mathrm{rad}$. The torque observer gain matrices were selected as $\boldsymbol{K_f} = 10 \times \mathrm{diag}[5;4]\,\mathrm{N\,m/rad}$ and $\boldsymbol{K_l} = 0.5 \times \mathrm{diag}[5;4]\,\mathrm{N\,m/(\,rad\,s)}$. In the operational space, the location of the virtual plane was described at $[0,\infty)\,\mathrm{m}$ in the X and $[-0.2,-\infty)\,\mathrm{m}$ in Y directions. The gain matrices for spring and damper were selected as $\boldsymbol{K_s} = 15 \times \boldsymbol{I_2}\,\mathrm{N/\,m}$ and $\boldsymbol{K_d} = 5 \times \boldsymbol{I_2}\,\mathrm{N\,s/\,m}$, respectively. The gain matrix for the null-space controller was selected as $\boldsymbol{K_{null}} = 2 \times \boldsymbol{I_3}\,\mathrm{N\,s}$.

Fig.s 4-9 present the results of the experiment study. Fig. 4 shows the end-effector tracking positions of the master robot and virtual slave. From a different perspective, Fig. 5 shows the end-effector trajectories of master robot and virtual slave in the X and Y translational directions. As seen in Fig.s 4 and 5, the end-effector positions of the master robot and virtual slave in the X and Y directions seem different due to the kinematic dissimilarity with different link lengths and the movements in the different work-space with their own initial joint configurations. However, as the most important result, it is obviously seen that the virtual slave's end-effector accurately tracks the master robot's end-effector at absolute value. From Fig. 6, it is confirmed that the coordination errors based on the end-effector trajectory trackings of the virtual slave and the master robot are less than 1 mm in both the X and Y translational directions. The control input torques applied on 2 joints of the master robot and 3 joints of the virtual slave are presented in Fig. 7. As it is observed, the control input torques are considerably less than the maximum continuous torque 2.2 N m at nominal position for PHANToM device. Fig. 8 presents estimates of human

torque $\hat{\tau}_{F_1}$ acting on the master robot and the model of environmental torque feed-back τ_{f_2} affecting the virtual slave. From Fig.s 7 and 8, it is observed that when the virtual slave is penetrating into the virtual plane as shown in Fig. 5, depending on the penetration depth and speed the environmental interaction force of the virtual slave is reflected back to the human operator at the same time with a certain proportion. Therefore, as the objective of the passive-decomposition based control method, safe physical interactions could be realized when the human operator uses the master robot and the slave robot is affected by the remote environment. As shown the joint positions of the virtual slave in Fig. 9, it is obviously seen that the secondary task was achieved since $\theta_{2.2}$ is entirely close to $\theta_{2.3}$.

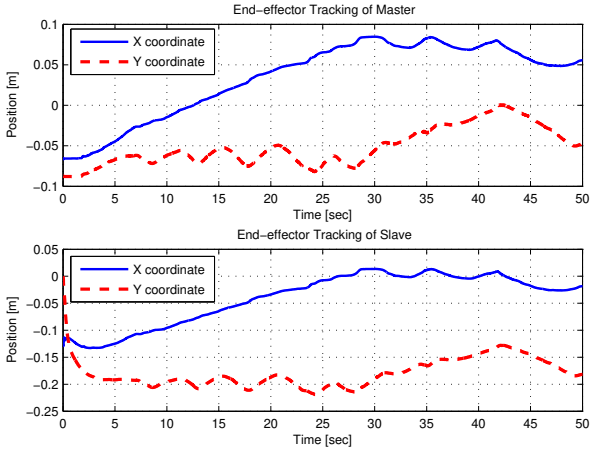

Fig. 4. End-effector tracking positions of the master robot (top) and the virtual slave (bottom).

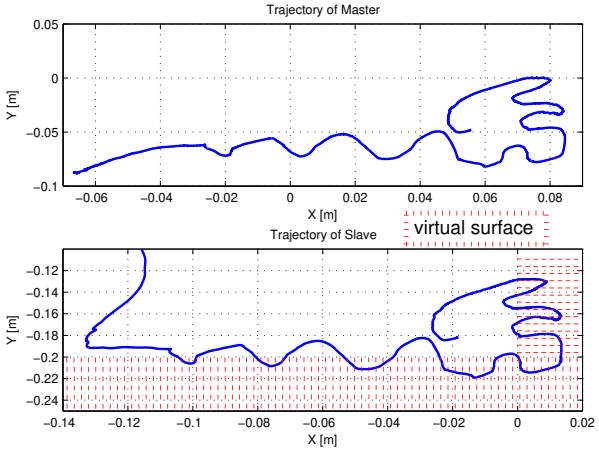

Fig. 5. End-effector trajectories on X-Y directions of the master robot (top) and the virtual slave (bottom).

6. DISCUSSION

Compared to the other passive decomposition based joint-space control approaches in the literature (Li and Lee, 2003; Lee and Li, 2005, 2007; Lee et al., 2013; Durbha and Li, 2019; Lee et al., 2020), the proposed passivity-based decomposing approach for operational space control

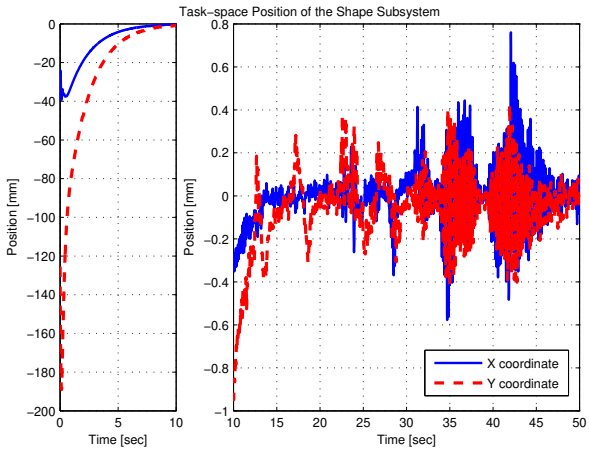

Fig. 6. Operational space positions of shape sub-system.

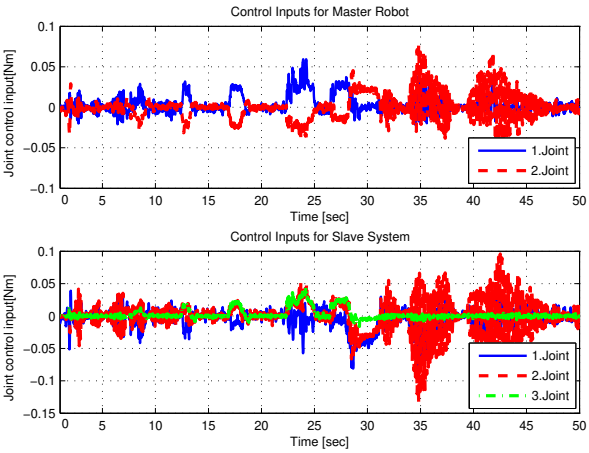

Fig. 7. Joint control inputs for the master robot (top) and the virtual slave (bottom).

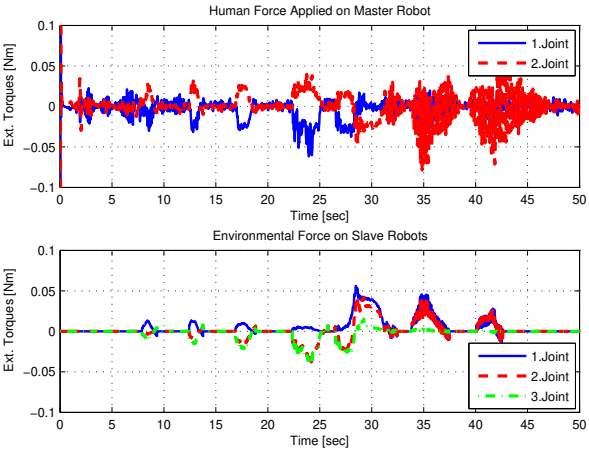

Fig. 8. Estimates of human torque $\hat{\tau}_{F_1}$ (top) and model of environmental torque τ_{f_2} (bottom).

can be applied to the kinematical redundant bilateral tele-operation systems. It should be noted that the advantage of kinematic redundancy in the slave robot was used for the first time in this study and that a subtask target was

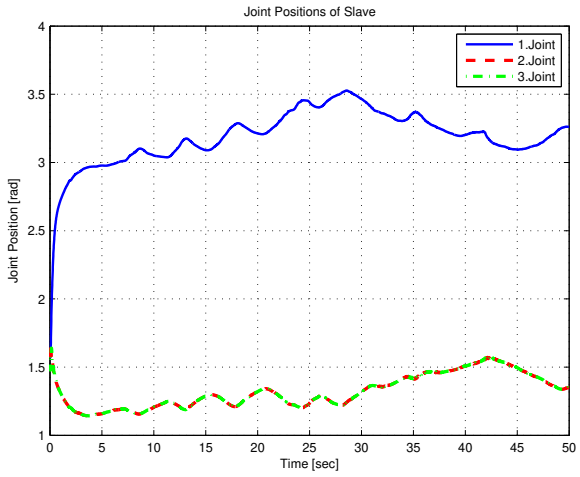

Fig. 9. Joint positions of virtual slave.

achieved for the bilateral tele-operation systems based on passive decomposition. Since the kinematics of the master and slave robots are usually different in terms of the dof in most tele-operation applications, the proposed approach has made an important contribution to the development of the passive decomposition methods. On the other hand, compared to the other operational space control methods for kinematical redundant tele-operation systems in the literature (Hwang and Hannaford, 1998; Nath et al., 2009; Liu and Chopra, 2011; Kapadia et al., 2012; Aldana et al., 2018), the proposed approach provides a referenced general movement of the closed-loop tele-operation system with the passivity of the safe physical human-robot and robot-environment interactions, as well as solving the kinematic redundancy and providing coordination between the end-effector positions of the master and slave robot arms.

7. CONCLUSION

In this study, a passivity-based decomposing method was developed for operational space control of a bilateral tele-operation system consisting of a non-redundant master robot and a redundant slave robot. By designing a non-square decomposition matrix, the redundant closed-loop tele-operation system was virtually decomposed into shape/locked sub-systems. The shape/locked sub-system controllers were then designed to ensure the coordination between the end-effectors of the master and slave robots in the operational space and to achieve the referenced general movement for the bilateral tele-operation system with safe physical interactions. By using the redundancy of the slave robot, to perform a secondary task, the slave controller was also integrated with a null-space control input to decrease the gradient function depending on the slave system's joint positions. To demonstrate the performance of the proposed approach, an experiment was carried out using a non-redundant PHANToM robot arm (master) and a redundant 3-dof robot arm model (slave). The experiment results confirmed the mathematical development of the passivity-based decomposing method for operational space control of kinematical redundant tele-operation systems.

ACKNOWLEDGEMENTS

This work was supported by TUBITAK project no. 113-E-147.

REFERENCES

Aldana, C.I., Cruz, E., Nuño, E., and Basañez, L. (2018). Control in the operational space of bilateral teleoperators with time-delays and without velocity measurements. *IFAC PapersOnLine*, 51(13), 204–209.

Chang, P.H. and Kim, J. (2012). Telepresence index for bilateral teleoperations. *IEEE Transactions on Systems, Man, and Cybernetics*, 42(1), 81–92.

Courreges, F., Vieyres, P., Poisson, G., and Novales, C. (2005). Real-time singularity controller for a teleoperated medical echography robot. In *IEEE/RSJ International Conference on Intelligent Robots and Systems*, 2222–2227.

Dasdemir, J. and Zergeroglu, E. (2015). A new continuous high-gain controller scheme for a class of uncertain nonlinear systems. *Int. J. of Robust and Nonlinear Control*, 25(1), 125–141.

Durbha, V. and Li, P.Y. (2019). Energetically passive bilateral teleoperation of a pneumatic crawling robot. In *Symposium on Fluid Power and Motion Control*, 1–10.

G. Frazelle, C., Kapadia, A., and Walker, I. (2018). Developing a kinematically similar master device for extensible continuum robot manipulators. *Journal of Mechanisms and Robotics*, 10(2), 025005.

Hokayem, P.F. and Spong, M.W. (2006). Bilateral teleoperation: An historical survey. *Automatica*, 42(12), 2035–2057.

Houssem, S., Laribi, M.A., Zeghloul, S., and Arsicault, M. (2018). On the development of a new master device used for medical tasks. *Journal of Mechanisms and Robotics*, 10(4), 044501.

Hwang, D.Y. and Hannaford, B. (1998). Teleoperation performance with a kinematically redundant slave robot. *The International Journal of Robotics Research*, 17(6), 579–597.

Kapadia, A.D., Walker, I.D., and Tatlicioglu, E. (2012). Teleoperation control of a redundant continuum manipulator using a non-redundant rigid-link master. In *International Conference on Intelligent Robots and Systems*, 3105–3110.

Lawrence, D.A. (1993). Stability and transparency in bilateral teleoperation. *IEEE Transactions on Robotics and Automation*, 9(5), 624–637.

Lee, D., Franchi, A., Son, H.I., Ha, C., Bülthoff, H.H., and Giordano, P.R. (2013). Semiautonomous haptic teleoperation control architecture of multiple unmanned aerial vehicles. *IEEE/ASME Transactions on Mechatronics*, 18(4), 1334–1345.

Lee, D. (2004). *Passive decomposition and control of interactive mechanical systems under coordination requirements*. Phd dissertation, Univ. Minnesota, Minneapolis, MN, USA.

Lee, D. and Li, P.Y. (2005). Passive bilateral control and tool dynamics rendering for nonlinear mechanical teleoperators. *IEEE Transactions on Robotics*, 21(5), 936–951.

Lee, D. and Li, P.Y. (2007). Passive decomposition approach to formation and maneuver control of multiple rigid bodies. *J. of Dynamic Systems, Measurement, and Control*, 129(5), 662–677.

Lee, S., Li, P.Y., and Eskilsson, F. (2020). Energetically passive multi-degree-of-freedom hydraulic human power amplifier with assistive dynamics. *IEEE Transactions on Control Systems Technology*, 28(4), 1296–1308.

Lewis, F., Dawson, D., and Abdallah, C. (2003). *Robot Manipulator Control: Theory and Practice*. Marcel Dekker, New York, NY, USA.

Li, P.Y. (1998). Passive control of bilateral teleoperated manipulators. In *Proceedings of the American Control Conference*, volume 6, 3838–3842.

Li, P.Y. and Lee, D. (2003). Passive bilateral feedforward control of linear dynamically similar teleoperated manipulators. *IEEE Tr. on Robotics and Automation*, 19, no.3, 443 – 456.

Liu, Y.C. and Chopra, N. (2011). Semi-autonomous teleoperation in task space with redundant slave robot under communication delays. In *International Conference on Intelligent Robots and Systems*, 679–684.

Lozano, R., Maschke, B., Brogliato, B., and Egeland, O. (2000). *Dissipative Systems Analysis and Control: Theory and Applications*. Springer-Verlag New York, Inc., Secaucus, NJ, USA.

McIntyre, M., Dixon, W., Dawson, D., and Tatlicioglu, E. (2006). Passive coordination of nonlinear bilateral teleoperated manipulators. *Robotica*, 24(4), 463–476.

Muradore, R. and Fiorini, P. (2016). A review of bilateral teleoperation algorithms. *Acta Polytechnica Hungarica*, 13(1), 191–208.

Nakanishi, J., Cory, R., Mistry, M., Peters, J., and Schaal, S. (2008). Operational space control: A theoretical and empirical comparison. *Int. J. of Robotics Research*, 27(6), 737–757.

Nath, N., Tatlicioglu, E., and Dawson, D.M. (2009). Teleoperation with kinematically redundant robot manipulators with sub-task objectives. *Robotica*, 27(7), 1027–1038.

Nuno, E., Basanez, L., and Ortega, R. (2011). Passivity-based control for bilateral teleoperation: A tutorial. *Automatica*, 47(3), 485–495.

Nygaard, A. (2008). *High-Level Control System for Remote Controlled Surgical Robots*. Master's thesis, Norwegian University of Science and Technology, Trondheim, Norway.

Rao, C.R. and Mitra, S.K. (1971). *Generalized Inverse of Matrices and Its Applications*. John Wiley & Sons, New York, NY, USA.

Siciliano, B. (1990). Kinematic control of redundant robot manipulators: A tutorial. *J. Intelligent and Robotic Systems*, 3(3), 201–212.

Spong, M. and Vidyasagar, M. (1989). *Robot Dynamics and Control*. John Wiley & Sons Inc., New York, NY, USA.